IEEE Access
Multidisciplinary ⋮ Rapid Review ⋮ Open Access Journal

Received September 10, 2020, accepted December 10, 2020, date of publication December 18, 2020,
date of current version January 4, 2021.

Digital Object Identifier 10.1109/ACCESS.2020.3045701

TBM-Mounted Seismic Ahead-Prospecting for Fast Detecting Anomalous Geology Ahead of Tunnel Face

LICHAO NIE[1], WEI ZHOU[1,2], XINJI XU[1,2], KAI WANG[3], LEI CHEN[1,2], ZHENGYU LIU[1], AND YAO LI[1]

[1]Geotechnical and Structural Engineering Research Center, Shandong University, Jinan 250061, China
[2]School of Qilu Transportation, Shandong University, Jinan 250061, China
[3]Qilu Transportation Development Group Company Ltd., Jinan 250101, China

Corresponding author: Xinji Xu (xuxinji1990@163.com)

This work was supported in part by the National Key Research and Development Plan under Grant [2016YFC0401801], and in part by the Science & Technology Program of Department of Transport of Shandong Province under Grant [2019 B47_2].

ABSTRACT Although performing tunnel excavation using tunnel boring machines (TBMs) is rapid, it is susceptible to the unexpected geological changes located in front of the tunnel face. Seismic detection methods are useful to detect local geological conditions in front of the tunnel face. However, manual detection is time consuming and may interfere in realizing rapid excavation by TBMs. Therefore, this study proposes an automated seismic detection system that is mounted on a TBM for rapidly imaging anomalous zones in front of the tunnel face. The system consists of an automated data acquisition system and a data processing system. The automated data acquisition system allows reducing the data acquisition time. To reduce the data processing time, the data processing system images the anomalous zones based on a modified Coppens' method. The proposed system has been mounted on TBMs and verified based on field tests.

INDEX TERMS Ahead prospecting in TBM tunnel, automated seismic detection system, automated data acquisition system, automated first-arrival picking, detection time reduction.

I. INTRODUCTION

With the rapid development of tunneling worldwide, using tunnel boring machines (TBMs) has become a favorable option when planning an excavation. In comparison with the conventional tunneling method (drilling and blasting), TBMs can provide a safe environment and a particularly high excavation speed, thus reducing the cost and the construction cycle [1]–[3]. However, TBMs are susceptible to the unknown geological changes located in front of the tunnel face [4]. An unexpected adverse geology could lead to disasters such as water/mud inrush resulting in delay or even casualties during the construction of a tunnel. For example, the Zagros water transfer tunnel encountered a great geological event with unpredicted and unforeseeable collapse, which caused the jamming of the TBM cutterhead and shield [5]. Hence, the geological conditions in front of the tunnel face should be explored in advance to ensure the excavation speed and safety of the TBMs. The geophysical exploration method, which is a non-destructive method, has the advantages of short detecting time and low cost, and is widely used in engineering investigation [6], [7]. By conducting geophysical exploration method, the distribution of the anomalous zones can be obtained [8], [9]. Therefore, researchers try to perform geophysical exploration in tunnel for detecting anomalous zones ahead of the tunnel face [6]. And ahead-prospecting methods have been proved to be an effective tool to predict the local geological conditions in front of the tunnel face, which is helpful for making construction decisions on disaster prevention [10], [11]. Thereby, the downtimes and safety risks during tunneling can be decreased. Geophysical exploration methods frequently used in predicting local geophysical condition in front of the tunnel face include three types of detection approaches to be relying on: 1) the elastic differences in the physical properties (Vp, Vs and density) using methods like Tunnel Seismic Prediction (TSP) and True Reflection Tomography (TRT) [12], [13]; 2) change in the magnetic field caused by the medium using method like Ground Penetrating Radar (GPR) [14] and Transient electromagnetic (TEM) [15]; 3) change in the shape of the electrical field generated by the

The associate editor coordinating the review of this manuscript and approving it for publication was Jenny Mahoney.

medium using method like electrical resistivity method and induced polarization (IP) method [6], [16]. However, there is such a large TBM machine in the TBM tunnel that may produce heavy electromagnetic interference which makes it hard for TEM and GPR to be adopted in TBM environment [17] and we have not found any application case of TEM and GPR for ahead-prospecting in TBM tunnel environment described in the literature. Many researchers have improved the electrical resistivity method and IP method in drilling and blasting tunnel and successfully applied them in TBM environment [4], [18], [19]. However, resistivity method and IP method are more effective for detecting water-bearing structure than detecting integrity of the rock mass. Among the above-mentioned 3 types of approaches, seismic method is a common used ahead-prospecting method with the advantages of relatively deep penetration range and high spatial resolution [20]. In this method, seismic waves are excited in a tunnel, and the reflection generated by the anomalous zones is recorded by receivers placed along the tunnel wall. By processing the seismic records, the fault zones, lithological boundaries, or large erratic blocks in front of the tunnel face can be detected [21]. Numerous detection systems are based on the seismic detection method. OYO Company developed the horizontal seismic profiling (HSP) method [22], setting shot points and receivers on two sides of a tunnel to facilitate the precision of the reflector position. Amberg Measuring Technique Company (Switzerland) developed the tunnel seismic prediction (TSP) method using an explosion source, which has numerous applications [12], [13]. NSA Engineering Company (USA) developed the true reflection tomography (TRT) technology, whose prediction range can be 60–150 m according to the geology conditions [10], [23]. Currently, most existing seismic ahead-prospecting systems require stopping the excavation for several hours for measuring coordinates and installing sensors on the tunnel face/side walls or to drill boreholes to insert measurement devices [3]. These flow paths are time consuming which may delay the construction. Concurrently, to obtain the distribution of the adverse geology in front of the tunnel face, the original seismic data should be processed. In most cases, data processing of the tunnel seismic data is based on the migration method. This method conventionally requires picking first arrivals of the direct waves in all the shot records. However, manual picking methods involve humans to decide the location to pick the first arrival on each seismic trace, which is time consuming [24]. Therefore, current seismic detecting systems are typically employed in tunnels being excavated by the drilling and blasting method. Under the constraints of rapid tunnel construction in TBM tunnels, the data acquisition and processing in the applied seismic detection methods should be completed within a short time. The common seismic method applied to a tunnel excavated by the drill and blast method can satisfy the demand of rapid TBM construction only after improvement. Recently, Tunnel Seismic While Drilling (TSWD) method has been proposed for predicting anomalous zones ahead of tunnel face and TBM tunnels. However, the traditional observed system of TSWD install the geophones on the ground surface [25], which is inconvenient for tunnels with large buried depth or tunnel length.

Attempts have been made to mount seismic detection systems on TBMs to perform the data acquisition quickly and conveniently. Li presented a comprehensive advanced geological detection system including multifunctional combination methods mounted on TBM [26]. The German Research Centre for Geoscience developed the integrated seismic imaging system (ISIS), in which the seismic sources are arranged at the gripper, whereas the geophones are set on the tips of the rock anchors. ISIS demonstrates the feasibility of TBM-mounted seismic detecting systems; therefore, tunnel seismic ahead-prospecting systems integrated with TBMs have become a major development trend [17]. Regarding seismic data procession, the development of computers has led to the proposal of automated computer-based algorithms to reduce the processing time [27]–[29]. As opposed to determining the signal advent by visual inspection of the amplitudes and waveform changes, an automatic picking method is based on machine picking in compliance with certain criteria, which is more efficient than manual picking.

In this study, we focused on reducing the time consumption of seismic detection to clarify the distribution of the adverse geology in front of a tunnel face without interfering in the TBM construction process. To reduce the time spent on data acquisition, a TBM-mounted automated seismic data acquisition system was proposed. The concept was to utilize automated machinery to reduce the time consumption of data acquisition with minimal steps and labor. In addition, an automated method for picking the first arrivals of the direct waves based on the energy ratio was presented to reduce the time spent on data processing. By combining the automated data acquisition system and automated picking method, the detection can be completed during the interval of a construction. Therefore, the distribution of the adverse geology in front of the tunnel face could be clarified in advance without interfering in the construction progress.

The remaining sections of this paper are organized as follows: The TBM-mounted automated data acquisition system is presented in Section 2. In Section 3, the processing method by the automated picking of the first arrivals of the direct waves for detecting adverse geology from the datasets acquired by the data acquisition system is described. To further verify the detecting method, the system was mounted on a TBM in China, and the results are discussed in Section 4. The conclusions are provided in Section 5.

II. AUTOMATED DATA ACQUISITION SYSTEM

One of the main tasks of this study was to reduce the time consumption of acquisition of the seismic data. Therefore, to satisfy the requirement of rapid construction by TBMs, an automated data acquisition system is proposed to be mounted on TBMs (Fig. 1). The automated data acquisition system consisted of a master control system, a hydraulic

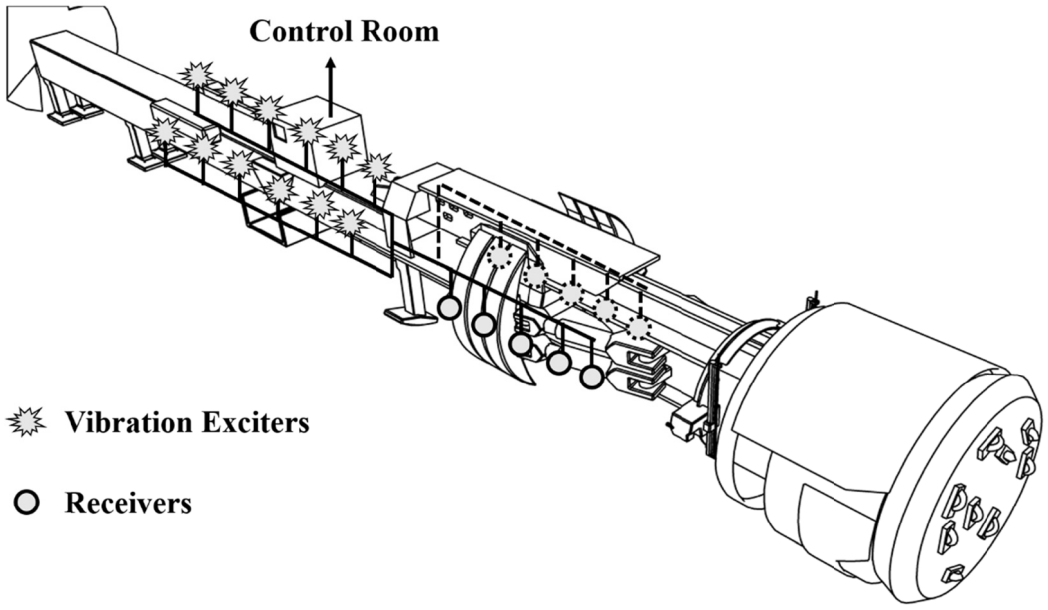

FIGURE 1. Set-up of a seismic detection system mounted on an open TBM.

system, vibration exciters, receivers, and a computer (Fig. 2). These devices can rapidly excite stable seismic waves and then collect and store the seismic signals for further processing

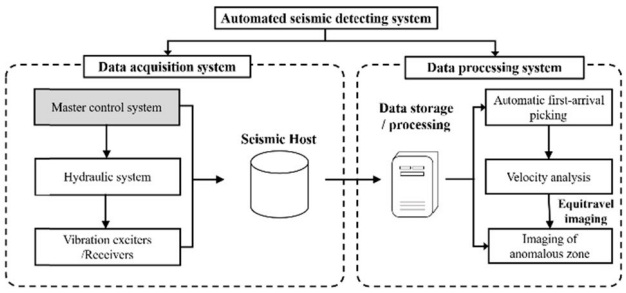

FIGURE 2. Schematic of the integrated detection system. This system can detect the anomalous zones present in front of a tunnel face without interfering in the TBM construction process. The data acquisition system can excite seismic waves using automatic machinery, whereas the data processing system can pick first arrivals automatically and then image the anomalous zones in front of the tunnel face rapidly.

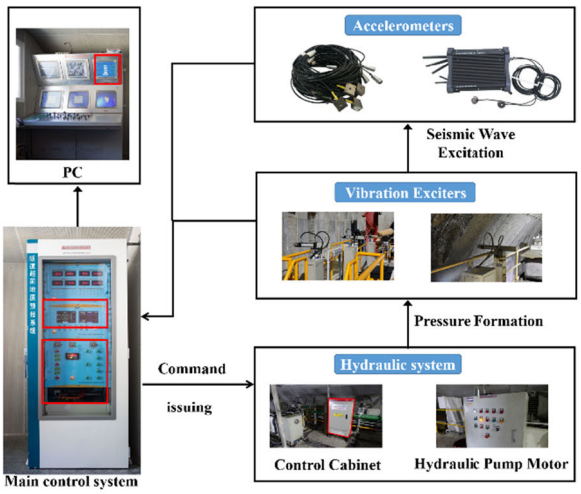

FIGURE 3. TBM-mounted data acquisition system. The hydraulic system is controlled by the master control system to generate stable high-energy pulses up to 21 MPa. The pressure causes the vibration exciters to hammer the surrounding rock to generate seismic waves and ensure that each seismic wave has sufficient energy to propagate.

- The master control system includes a seismic host and a control panel, which is installed in the control room (Fig. 3). Using the control panel, the seismic host can be commanded to control the entire acquisition system for realizing fast seismic wave excitation and data acquisition.
- The hydraulic system is connected to the main control system and the vibration exciters. It is controlled by the master control system to generate stable high-energy pulses up to 21 MPa. The pressure causes the vibration exciters to hammer the surrounding rock to generate seismic waves and ensure that each seismic wave has sufficient energy to propagate. Typically, the hydraulic system excites a seismic wave thrice at each shot point. Compared with the common manual seismic wave excitation method, the time spent on repeated excitation required owing to the occasional insufficient manual exciting energy is avoided. Concurrently, the time spent on drilling and charging is saved relative to that on the explosion excitation.
- The vibration exciters are mounted using the columns on the TBM second floor, and the type of trigger is a hammer (Fig. 3). Fixing the vibration exciters to the

TBM avoids the process of measuring the coordinates of the shot points. In seismic detection, the coordinate measurement of a shot point is closely related to the calculation of the direct wave velocity. When conducting common seismic detection, surveyors require more than 30 min for measuring the coordinates of the shot points using unique equipment. Different from the common seismic detection, the vibration exciters of the proposed automated data acquisition system maintain the same relative position during the excavation of a tunnel because of being mounted on the TBM. The relative coordinates of the shot points are measured when installing the vibration exciters and then used in the data processing. Thus, the time required for measuring the coordinates of the shot points is saved.

- The receivers are installed on the side wall behind the tunnel face and connected to the seismic host for collecting the seismic signals. The sampling interval is 0.1 ms, and the sampling length is 512–8192 ms.
- The computer is installed in the control room for displaying and storing the collected seismic signals. Moreover, the processing software is installed on the computer. Thus, the detection results can be transmitted to the constructors immediately after rapidly processing the acquired data.

During seismic detection, the hydraulic system forms pressure pulsation for the vibration exciters after receiving the command from the master control system. Then the vibration exciters hammer the sidewall and excite the incident seismic wave. When the seismic waves encounter adverse geologies (faults, joint, and so on), the waves are reflected and then received by the geophones [13]. Finally, the seismic signals, including the exciting and receiving signals, are collected by the seismic host and stored in the computer (Fig. 2). The proposed data acquisition system can complete the data acquisition in 30 min compared to the several hours required to install sensors in most existing ground prediction systems [3].

III. METHODOLOGY

The locations of the anomalous zones can be obtained after data processing. One of the most used methods for seismic data processing is the migration imaging method. This method conventionally requires picking the first arrivals of the direct waves on each source–receiver pair, for the velocity analysis, which is important to determine the source–reflector–receiver distance [24], [30]. However, following factors makes manual picking time consuming (1) The amplitudes of both the signal and noise is different from trace to trace. (2) Background noise may swamp the early received signal and makes eyes hard to recognize the first arrival [31]. Therefore, these factors make manual picking time consuming can barely meet the requirement of rapid excavation by TBMs. For example, 120 traces can be acquired by a configuration including 12 vibration exciters and 10 receivers, which may require a time of more than 20 min in case of manual picking. Hence, automatic picking techniques are used to pick the first arrivals to achieve high efficiency. In this section, we propose an automatic picking method for the velocity analysis. Thus, the time spent on seismic data processing can be reduced by more than 50%.

A. AUTOMATIC FIRST-BREAK PICKING

During the last few decades, numerous automatic first arrival picking methods have been developed [32]. In recent years, neural network algorithm and fractal-dimension-based method have been adopt to first arrival picking [33]. And approaches based on detecting the sudden energy increasing are one of the important and classic way to identify the first arrival. The criteria of such automatic picking method are similar to those of a manual picking method. For example, Spagnolini proposed an adaptive picking method on the detection abrupt change of energy [34]. Coppens [35] proposed a first-arrival picking method to compare the energy contained in a window ranging from zero time to the end of the window, as expressed in Eq. (1).

$$F(\tau) = \int_{\tau-L}^{\tau} S^2(t)dt \Big/ \int_{0}^{\tau} S^2(t)dt, \tag{1}$$

where L is the width of the small running window and determined according to the apparent period of the first arrival and $S(t)$ is the amplitude at time t. The first arrival is determined as the τ_0 of the maximum of $F(\tau)$. As stated by Coppens [35], this method is successful when the signal-to-noise ratio is sufficiently high. However, the requirement of numerous construction machinery and construction operations makes the noise environment in a TBM tunnel complex. For example, the reinforcement works for newly exposed surrounding rock such as a steel arch support, bolt support, shotcrete, and machinery (e.g., a ventilation system and water pump may generate strong noise). These noises may cause the incorrect picking of the first arrival wave. Sabbione and Velis [32] proposed a modified Coppens' method (MCM) to improve the automatic picking performance when the seismic record is interfered by noise (Fig. 4). The amplitude is initially normalized, and the energy of the seismic trace, $S(t)$, within two nested windows (Fig. 4) is calculated using Eq. (2) and Eq. (3) [35].

$$E_{MCM1}(t) = \sum_{i=t-n_l+1}^{t} s_i^2, \tag{2}$$

$$E_{MCM2}(t) = \sum_{i=1}^{t} s_i^2 \tag{3}$$

where n_l is the length of the leading window and selected a priori. Further, the energy ratio is calculated using Eq. (4) [35].

$$F_{MCM}(t) = E_{MCM1}(t)/(E_{MCM2}(t) + \beta), \tag{4}$$

where β is a stabilization constant to reduce the influence of the noise. This is effective because the energy of a long window is small when the value of t is small, and the stabilization constant can stabilize the energy ratio oscillation instead

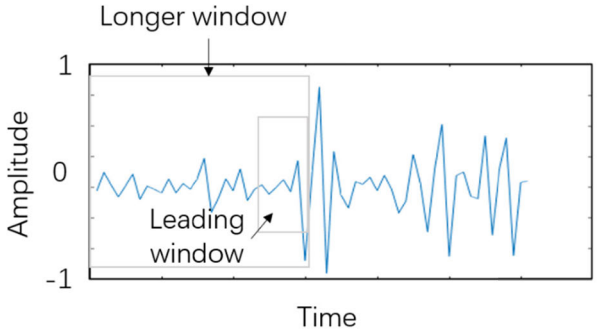

FIGURE 4. Nested windows used in the calculation of the energy ratio.

of picking wrong t_0. However, as stated by Sabbione and Velis [32], there still might be some bad traces or wrong picks. Hence, an improved MCM method adopting an iteration stratagem to correct mispicking is proposed in this section.

The basic concept of the improved MCM is to improve the first arrival picking within an iteration, for which an iteration method is adopted. After picking the initial first arrival according to the MCM method, the initial first arrival time of each source–receiver pair is obtained. Meanwhile, the relative coordinates of the sources and receivers are fixed as state in Section 2, and the distance of each source–receiver pair are easily calculated. Then, the least-square linear regression is applied to the initial first picking results of each source–receiver pair (Fig. 5). For example, there would be totally N results for N source–receiver pair, and the regression line is calculated based on the N results. Then the Euclidean distance between each result and the regression line is calculated, the long window energy is recalculated based on the distance, and the first arrival is re-picked until the distance between each result and the regression line is less than 2σ.

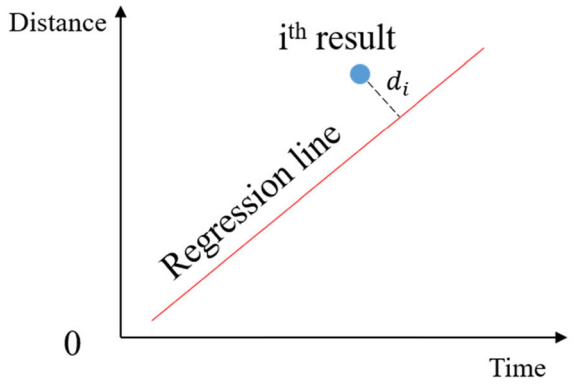

FIGURE 5. Determination of the Euclidean distance between each first arrival picking result and the regression line for calculating the weight factor.

For convenience, the seismic amplitudes are normalized to $(-1,1)$ and the seismic traces are divided into several windows. The energy ratio is calculated as Eq. (5) [32].

$$ER\,(t) = E_1\,(t)/(E_2\,(t) + \beta) \tag{5}$$

where β is a stabilization constant similar to that in the MCM, $E_1\,(t)$ is the energy of the leading window calculated by MCM method as expressed in Eq. (2), and $E_2\,(t)$ is calculated using Eq. (6).

$$E_2\,(t) = \sum_{i=1}^{t} \xi_i \cdot s_i^2, \tag{6}$$

where s_i is the energy of the i_{th} window and ξ_i is the weight factor of the i_{th} window calculated by Eq. (7).

$$\xi_i\,(t) = b_1\,(b_2 - t) \cdot d_i^2 + 1, \tag{7}$$

where b_1, b_2 remain constant during the iteration and are selected according to the experience, d_i is the Euclidean distance from the i_{th} model to the i_{th} regression line, and all the initial values of d_i are 0. The iterations continue until all the d_i are less than 2σ, where σ is the standard value of d_i.

A flowchart of the proposed method is presented in Table 1.

TABLE 1. Processing flow for the data processing.

Flowchart of the improved MCM method
1) Choose the leading window length, n_l , and the stabilization constant, β
2) Set j = 0, and calculate the distance between each receiver and shot point.
3) If j = 0,
Set $d_i = 0$, and compute the weight factor, ξ_i , using Eq. (7).
4) Else j >= 1,
Compute the weight factor using Eq. (7)
5) Calculate the energy ratio using Eq. (5) and determine the first arrival of each trace.
4) Use the least-squares regression to measure the direct wave velocity
5) Calculate the distance, d_i , from each result to the regression line
6) If $d_i < 2\sigma$,
Select τ_i as the first arrival time
7) If $d_i >= 2\sigma$,
Update distance d_i from each model to the regression line for the $(j+1)^{th}$ iteration.
8) j = j+1
9) end

B. MIGRATION IMAGING METHOD

The workflow of the seismic data processing is presented in Fig. 6. Initially, the data files are read and formatted. Then, integral transformations are performed on the seismic data for further analysis. The energy attenuation of the seismic waves and differences in the coupling may cause the amplitudes of the seismic signals to vary. Therefore, to facilitate the processing of the signals, the trace equalization method is adopted to balance the amplitude of each trace. Next, for velocity analysis, automatic first arrival picking is performed on each source–receiver pair, following which the velocity of an elastic wave can provide the basis for migration imaging and then the first arrivals are removed. To extract the useful

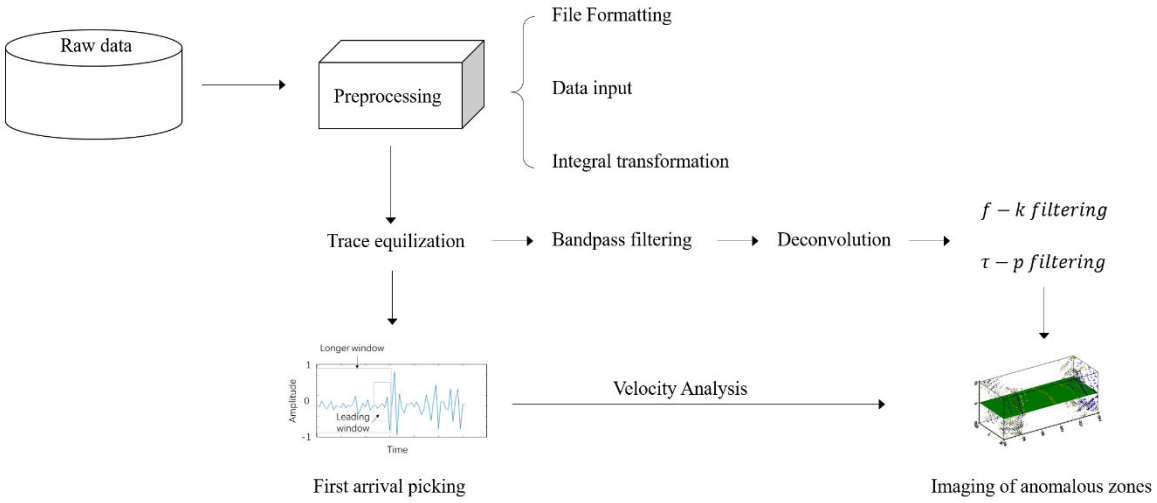

FIGURE 6. Framework of the seismic processing method for imaging anomalous zones.

signals, after the spectral analysis, the seismic signals are bandpass filtered and deconvoluted. Moreover, a combined filtering method based on the f–k and $\tau - p$ methods [17] is introduced to separate complex wave fields. Finally, the equitravel time plane algorithm, which generates an equitravel time ellipsoid for each source–receiver pair, is applied in this study [17], [36]. For several source–receiver pairs, the same number of ellipsoids can be obtained, and their common tangent plane forms a plane of reflection. Then the distribution of the reflection coefficients can be obtained in the imaging region. In this paper, the processing software proposed by Liu *et al.* [17] is adopted as the migration imaging method.

IV. RESULTS AND DISCUSSION

The Dali–Ruili Railway Project is located in Yunnan province in southwest China. It is the last section of the China–Myanmar International Railway in China, which makes it important to the development of Yunnan province. The Gaoligongshan Tunnel is the dominant engineering of the Dali–Ruili Railway Project with a buried depth of up to 1155 m and a length of 34.538 km, 13 km of which was constructed using an open TBM of 9 m in diameter. The Gaoligongshan Tunnel passes through the west of the Hengduan mountains on the southeastern edge of the Tibetan Plateau (TP), where the Yanshanian granite is affected by faults. A longitudinal section map illustrating the geological conditions of the Gaoligongshan Tunnel is presented in Fig. 7. To ensure the safe and rapid construction of the Gaoligongshan Tunnel, the constructors adopted the automated seismic detection system proposed in this paper. The detection was performed practically along the whole line of the tunnel during the daily downtime of the TBM excavation. As summarized in Table 2, the statistics exhibit that the proportion of the receiving valid signals and the time spent on the detection are related to the rock mass. To verify the efficacy of the proposed data processing method, two cases were conducted in the fault fracture zone and weathered zone, which are presented respectively.

A. EXPERIMENT1 AT MILEAGE OF D1k225+000

The field seismic detection was conducted at a mileage of D1k225+000, and the seismic data was acquired by the automated data acquisition system, by the method as described in Section 2, during the downtime of the tunnel excavation. The geological survey analysis revealed that the geological section mainly contained fault breccias distributed throughout it, and the rock mass had a relatively poor integrity. The seismic data were acquired by the automated data acquisition system, which is described in Section 2. Owing to the dry shotcrete, ten vibration exciters were selected as the seismic trigger points on both tunnel sidewalls, and four and five receivers were set on the right and left sidewalls, respectively.

The results of the automatic first arrival picking are similar to those of the manual picking method in most traces, as shown in Fig. 8. However, there are still some traces for which it is difficult to pick the actual first arrival, owing to the strong noise, and these traces are eliminated when calculating the direct wave velocity. The velocity of the direct waves calculated based on the automated first arrival picking method is 3500 m/s. By the data processing described in Section 3, approximately 30 min is required to process the seismic data, and the imaging result of reflection coefficient is presented in Fig. 9.

In the results, the areas with positive or negative reflections are usually represent the fractured or weathered zones. The strong reflections fall into two zones: A1 and A2. These two zones invade the tunnel approximately at mileages of D1k225+000 to D1k224+980 and of D1k224+935 to D1k224+900, respectively. Combined with the geological analysis, the fractured zones at the different mileages are interpreted as follows:

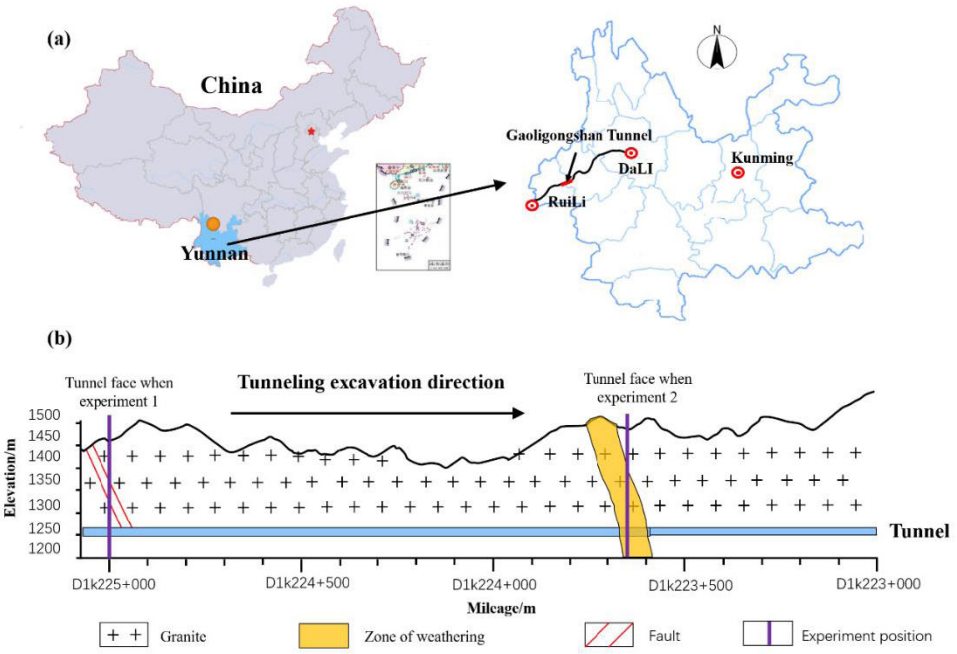

FIGURE 7. Sketch of the cross-section illustrating (a) the geographic location of the Gaoligongshan Tunnel and (b) geological longitudinal section map obtained by the surface geotechnical investigation for identifying the possible adverse geological zones and the experiment location.

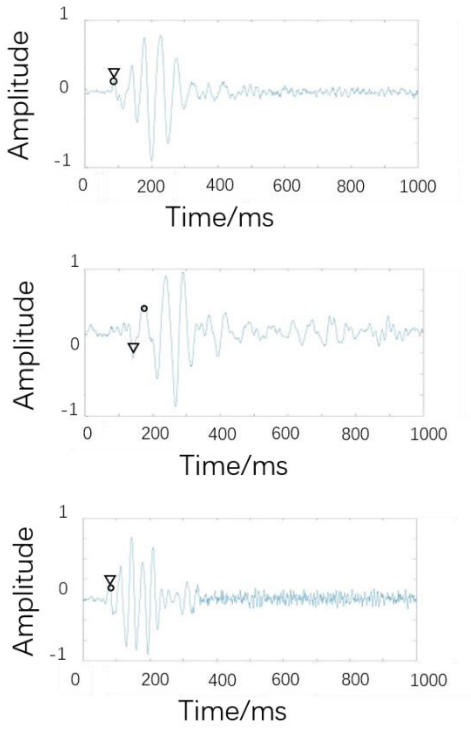

FIGURE 8. First arrival picking results of the automatic and manual picking methods. The circle represents the first arrival picking results of the manual picking method while the triangle represents the first arrival picking results of the automatic picking method.

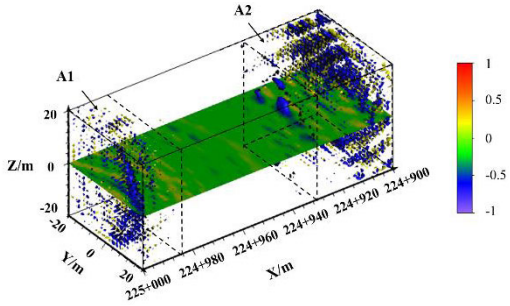

FIGURE 9. Seismic imaging result based on the automatic first arrival picking method at D1k225+000. The detecting depth is 100 m, the x-axis is parallel to the tunnel axis, the y-axis is parallel to the tunnel face, and the z-axis is perpendicular to the bottom of the tunnel.

- At mileages D1k225+000 to D1k224+980, there is an abnormal zone, Zone A1, which contains numerous strong reflections. Thus, we can expect that the rock mass of this zone is fractured and that partial rock masses are extremely poor, as determined by the lower RMR value than that for the rock exposed in the tunnel face.
- At mileages D1k224+980 to D1k224+935, the reflection is not remarkable. Thus, it is assumed that the rock mass of this zone is the same as that exposed in the tunnel face and is better than that in the previous 30 m.
- At mileages D1k224+935 to D1k224+900, there is an abnormal zone, Zone A2, which contains numerous strong reflections. Thus, it is assumed that an anomalous zone, such as fractured rock, with a lower quality ground, as indicated by the lower RMR value, is expected to be present in this area.

To verify the efficacy of the proposed first arrival picking method, the manual picking method is applied. The direct

wave velocity is 3400 m/s. When conducting manual first arrival picking, human tend to select a point which has an obvious amplitude change to avoid the influence of noise. However, the proposed automatic picking method selects the first arrival wave only based on the energy ratio. therefore, the elastic wave velocity obtained using it is higher than that derived based on the manual picking method. The imaging result is presented in Fig. 10.

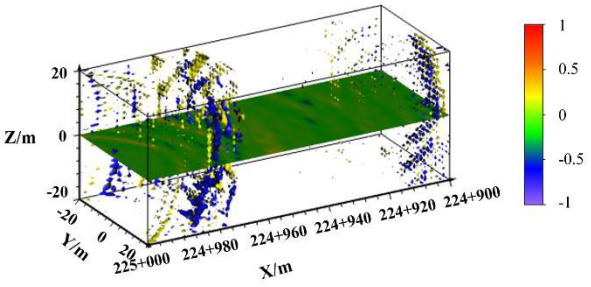

FIGURE 10. Seismic imaging result of the same seismic data as that in Fig. 9 based on the manual first arrival picking method instead of the automatic picking method at D1k225+000. The detection depth is 100 m, the x-axis is parallel to the tunnel axis, the y-axis is parallel to the tunnel and the tunnel face, and the z-axis is perpendicular to the bottom of the tunnel. It can be seen that the distribution of the anomalous zones is nearly the same as that in Fig. 9.

Comparing Figs. 9 and 10 exhibit that the imaging results obtained based on the automatic and manual picking methods are similar. To verify the efficacy of the proposed automated seismic detecting system, a geological sketch map was drawn during the tunneling. The imaging result and the geological sketch map are compared in Fig. 11. As shown in Fig.11, the predicting results of the anomalous zones A1, A1 coincide well with the excavation results. However, a small fault exposed at mileage of D1k224+970 and D1k 224+950 was not considered as an anomalous zone when interpreting. Actually, there no lithological changes at this mileage and the width of the fault is small. It was identified as a fault because there was a small misalignment between the hanging wall and footwall. Thus, the reflection of the fault is not as obvious as that of A1 and A2 as shown in Fig. 11(a). Meanwhile, the integrity of the surrounding rock between mileage of D1k224+970 and D1k 224+950 is better than that in the anomalous zones, which has little impact on engineering safety.

B. EXPERIMENT 2 AT MILEAGE OF D1k223+664

Another test was conducted at a mileage of D1k223+664. According to the geologic longitudinal section map provided by the geotechnical investigation performed on the ground, as presented in Fig 7, a weathered deep groove invades the tunnel trunk at mileages of D1k223+660 to D1k223+580. Consequently, this area may comprise of weathered rocks. The seismic data were also acquired by the automated data system, as described in Section 2. Ten vibration exciters were selected as the seismic trigger points on both the tunnel

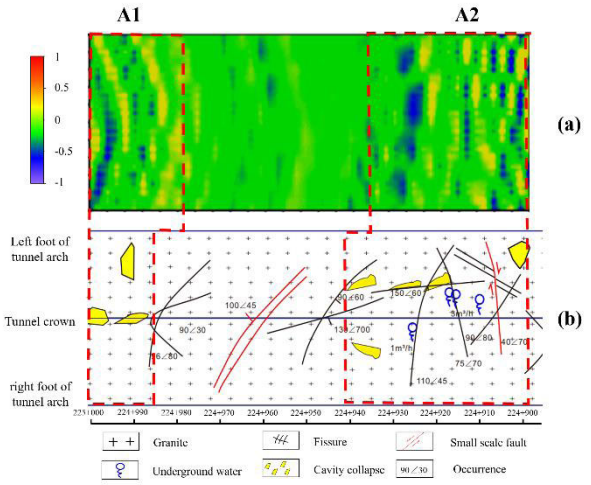

FIGURE 11. Comparison of the imaging results and the geological sketch map based on an actual excavation. (a) Imaging result obtained by the proposed system at mileages of D1k225+000 to D1k224+900 and (b) sketch map of the actual excavation at mileages of D1k225+000 to D1k224+900.

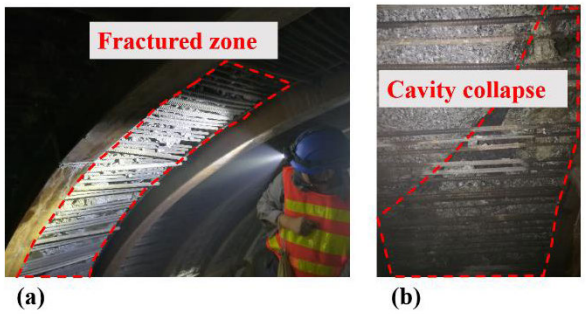

FIGURE 12. Fractured zones and cavity collapse during the excavation. (a) Fractured zone located at the left arch shoulder at mileages of D1k224+990 and (b) cavity collapse at D1k224+935.

sidewalls, and five receivers each were set on the right and left sidewalls.

The velocities of the direct waves calculated based on the automated first arrival picking method and manual first arrival picking method are 4800 m/s and 4500m/s, respectively. By the data processing described in Section 3, the imaging results of reflection coefficient obtained based on the automatic picking method are displayed in Fig. 13.

The strong reflections fall into three zones: A1, A2, and A3. These zones invade the tunnel approximately at mileages of D1k223+664 to D1k223+649, D1k223+620 to D1k223+599, and D1k223+584 to D1k223+564, respectively. Combined with the geological analysis, the fractured zones at the different mileages are interpreted as follows:

- At mileages of D1k223+664 to D1k223+649, D1k223+616 to D1k223+599, and D1k223+584 to D1k223+564, there are three abnormal zones, which contain numerous reflections. Thus, it is assumed that the rock masses of these three zones are fractured and are broken, suggesting that cavity collapse may occur during excavation in this area.

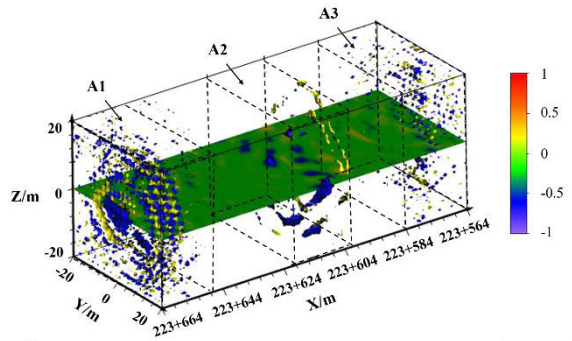

FIGURE 13. Seismic imaging result based on the automatic first arrival picking method at D1k223+664. The detecting depth is 100 m, the x-axis is parallel to the tunnel axis, the y-axis is parallel to the tunnel face, and the z-axis is perpendicular to the bottom of the tunnel.

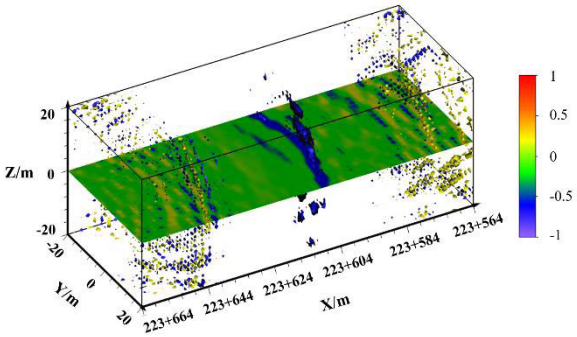

FIGURE 14. Seismic imaging results based on the manual first arrival picking method at D1k223+664. The detecting depth is 100 m, the x-axis is parallel to the tunnel axis, the y-axis is parallel to the tunnel face, and the z-axis is perpendicular to the bottom of the tunnel.

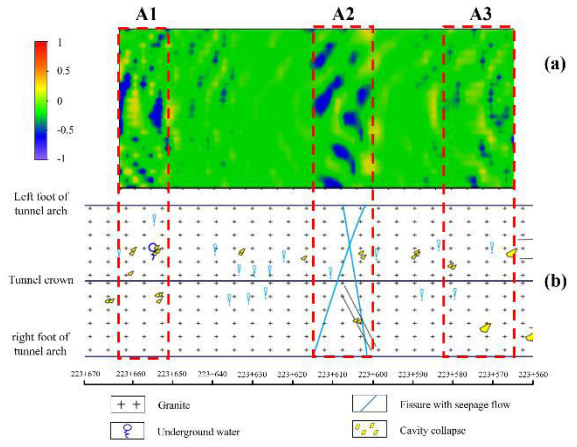

FIGURE 15. Comparison of the imaging result and the geological sketch map based on an actual excavation. (a) Imaging result of proposed system at mileage of D1k223+664 to D1k223+564; and (b) sketch map of the actual excavation at mileage D1k223+664 to D1k223+564.

- At mileages of D1k223+649 to D1k223+616 and D1k223+599 to D1k223+584, the reflection is not remarkable. Thus, we expect that the rock mass of this zone is the same as that exposed in the tunnel face.

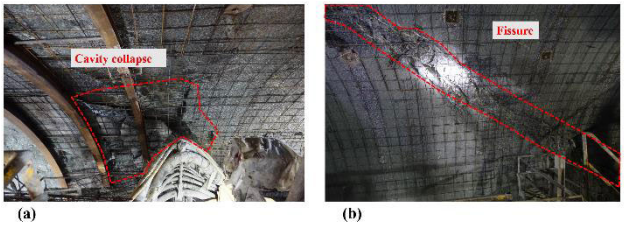

FIGURE 16. Cavity collapse and fissure during excavation. (a) Cavity collapse located at left arch shoulder at mileage of D1k223+655; (b) fissure at D1k223+605.

The imaging results based on the manual picking is depicted in Fig. 14, and they are consistent with those obtained by the automatic picking method.

To verify the efficacy of the proposed automated seismic detecting system, a geological sketch map was drawn during the tunneling. The imaging result and the geological sketch map are compared in Fig. 15.

V. CONCLUSION

This paper proposed an automated seismic prospecting system for a TBM that consisted of an automated data acquisition system and a data processing method based on an automatic first arrival picking method. The seismic waves were initially excited and received by the data acquisition system. Then, the first arrival was picked by the modified Coppens' method, and the least-square linear regression was conducted. Next, an iteration scheme that corrected the incorrect picking according to the distance between each model and the regression line was applied. Finally, equitravel imaging utilizing the obtained direct wave velocity was performed to acquire the distribution of the anomalous zones. Compared to the manual detecting method, the automated data acquisition system could reduce the time consumption of the seismic data acquisition and the automatic first arrival picking method could reduce that of the data processing. To further estimate the effectiveness of the proposed system, the proposed system was mounted on a TBM and validated by two field tests in Yunnan, China. The field test show that the proposed system could image the distribution of the anomalous zones without interfering in the TBM construction process, which could ensure safe and rapid TBM tunneling. In future work, a comprehensive detecting system mounted on a TBM using multiple geophysical methods should be proposed and further study of automatic anomalous zone identification must be conducted. It is expected that the findings reported in this paper will motivate such research in the future.

REFERENCES

[1] C. Zhou, T. Kong, Y. Zhou, H. Zhang, and L. Ding, "Unsupervised spectral clustering for shield tunneling machine monitoring data with complex network theory," *Autom. Construct.*, vol. 107, Nov. 2019, Art. no. 102924, doi: 10.1016/j.autcon.2019.102924.

[2] W. Sun, M. Shi, C. Zhang, J. Zhao, and X. Song, "Dynamic load prediction of tunnel boring machine (TBM) based on heterogeneous *in-situ* data," *Autom. Construct.*, vol. 92, pp. 23–34, Aug. 2018, doi: 10.1016/j.autcon.2018.03.030.

[3] L. Wei, D. R. Magee, and A. G. Cohn, "An anomalous event detection and tracking method for a tunnel look-ahead ground prediction system," *Autom. Construct.*, vol. 91, pp. 216–225, Jul. 2018, doi: 10.1016/j.autcon.2018.03.002.
[4] K. Schaeffer and M. A. Mooney, "Examining the influence of TBM-ground interaction on electrical resistivity imaging ahead of the TBM," *Tunnelling Underground Space Technol.*, vol. 58, pp. 82–98, Sep. 2016, doi: 10.1016/j.tust.2016.04.003.
[5] M. Bayati and J. K. Hamidi, "A case study on TBM tunnelling in fault zones and lessons learned from ground improvement," *Tunnelling Underground Space Technol.*, vol. 63, pp. 162–170, Mar. 2017, doi: 10.1016/j.tust.2016.12.006.
[6] S. Li, B. Liu, X. Xu, L. Nie, Z. Liu, J. Song, H. Sun, L. Chen, and K. Fan, "An overview of ahead geological prospecting in tunneling," *Tunnelling Underground Space Technol.*, vol. 63, pp. 69–94, Mar. 2017, doi: 10.1016/j.tust.2016.12.011.
[7] B. Liu, Y. Pang, D. Mao, J. Wang, Z. Liu, N. Wang, S. Liu, and X. Zhang, "A rapid four-dimensional resistivity data inversion method using temporal segmentation," *Geophys. J. Int.*, vol. 221, no. 1, pp. 586–602, Apr. 2020, doi: 10.1093/gji/ggaa019.
[8] S. Li, B. Liu, Y. Ren, Y. Chen, S. Yang, Y. Wang, and P. Jiang, "Deep-learning inversion of seismic data," *IEEE Trans. Geosci. Remote Sens.*, vol. 58, no. 3, pp. 2135–2149, Mar. 2020, doi: 10.1109/TGRS.2019.2953473.
[9] B. Liu, Q. Guo, S. Li, B. Liu, Y. Ren, Y. Pang, X. Guo, L. Liu, and P. Jiang, "Deep learning inversion of electrical resistivity data," *IEEE Trans. Geosci. Remote Sens.*, vol. 58, no. 8, pp. 5715–5728, Aug. 2020, doi: 10.1109/TGRS.2020.2969040.
[10] Y. Zhao, H. Jiang, and X. Zhao, "Tunnel seismic tomography method for geological prediction and its application," *Appl. Geophys.*, vol. 3, no. 2, pp. 69–74, Jun. 2006, doi: 10.1007/s11770-006-0010-7.
[11] W. Gao, L. Shi, J. Han, and P. Zhai, "Study on control water of Ordovician aquifer: A coal mine of Feicheng mining area, China," *Carbonates Evaporites*, vol. 35, no. 2, p. 48, Jun. 2020.
[12] A. Alimoradi, A. Moradzadeh, R. Naderi, M. Z. Salehi, and A. Etemadi, "Prediction of geological hazardous zones in front of a tunnel face using TSP-203 and artificial neural networks," *Tunnelling Underground Space Technol.*, vol. 23, no. 6, pp. 711–717, Nov. 2008, doi: 10.1016/j.tust.2008.01.001.
[13] S.-S. Shi, S.-C. Li, L.-P. Li, Z.-Q. Zhou, and J. Wang, "Advance optimized classification and application of surrounding rock based on fuzzy analytic hierarchy process and tunnel seismic prediction," *Autom. Construct.*, vol. 37, pp. 217–222, Jan. 2014, doi: 10.1016/j.autcon.2013.08.019.
[14] B. Liu, F. Zhang, S. Li, Y. Li, S. Xu, L. Nie, C. Zhang, and Q. Zhang, "Forward modelling and imaging of ground-penetrating radar in tunnel ahead geological prospecting," *Geophys. Prospecting*, vol. 66, no. 4, pp. 784–797, May 2018, doi: 10.1111/1365-2478.12613.
[15] G. Q. Xue, Y. J. Yan, X. Li, and Q. Y. Di, "Transient electromagnetic S-inversion in tunnel prediction," *Geophys. Res. Lett.*, vol. 34, no. 18, pp. 1–5, 2007, doi: 10.1029/2007GL031080.
[16] S. Li, S. Xu, L. Nie, B. Liu, R. Liu, Q. Zhang, Y. Zhao, Q. Liu, H. Wang, H. Liu, and Q. Guo, "Assessment of electrical resistivity imaging for pre-tunneling geological characterization—A case study of the Qingdao R3 metro line tunnel," *J. Appl. Geophys.*, vol. 153, pp. 38–46, Jun. 2018, doi: 10.1016/j.jappgeo.2018.03.024.
[17] B. Liu, L. Chen, S. Li, J. Song, X. Xu, M. Li, and L. Nie, "Three-dimensional seismic ahead-prospecting method and application in TBM tunneling," *J. Geotech. Geoenvironmental Eng.*, vol. 143, no. 12, Dec. 2017, Art. no. 04017090.
[18] J. Park, K.-H. Lee, J. Park, H. Choi, and I.-M. Lee, "Predicting anomalous zone ahead of tunnel face utilizing electrical resistivity: I. Algorithm and measuring system development," *Tunnelling Underground Space Technol.*, vol. 60, pp. 141–150, Nov. 2016, doi: 10.1016/j.tust.2016.08.007.
[19] S. Li, L. Nie, and B. Liu, "The practice of forward prospecting of adverse geology applied to hard rock TBM tunnel construction: The case of the Songhua River water conveyance project in the middle of Jilin Province," *Engineering*, vol. 4, no. 1, pp. 131–137, Feb. 2018.
[20] F. Cheng, J. Liu, N. Qu, M. Mao, and L. Zhou, "Two-dimensional pre-stack reverse time imaging based on tunnel space," *J. Appl. Geophys.*, vol. 104, pp. 106–113, May 2014, doi: 10.1016/j.jappgeo.2014.02.013.
[21] S. Jetschny, T. Bohlen, and A. Kurzmann, "Seismic prediction of geological structures ahead of the tunnel using tunnel surface waves," *Geophys. Prospect.*, vol. 59, pp. 934–946, Aug. 2011, doi: 10.1111/j.1365-478.2011.00958.x.
[22] T. Inazaki, H. Isahai, S. Kawamura, T. Kurahashi, and H. Hayashi, "Stepwise application of horizontal seismic profiling for tunnel prediction ahead of the face," *Lead. Edge*, vol. 18, no. 12, pp. 1429–1431, Dec. 1999, doi: 10.1190/1.1438246.
[23] R. Otto, E. Button, H. Bretterebner, and P. Schwab, "The application of TRT true reflection tomography at the unterwald tunnel," *Felsbau*, vol. 20, no. 2, pp. 51–56, 2002.
[24] W. A. Mousa, A. A. Al-Shuhail, and A. Al-Lehyani, "A new technique for first-arrival picking of refracted seismic data based on digital image segmentation," *Geophysics*, vol. 76, no. 5, pp. V79–V89, Sep. 2011, doi: 10.1190/geo2010-0322.1.
[25] L. Petronio, F. Poletto, and A. Schleifer, "Interface prediction ahead of the excavation front by the tunnel-seismic-while-drilling (TSWD) method," *Geophysics*, vol. 72, no. 4, pp. G39–G44, Jul. 2007, doi: 10.1190/1.2740712.
[26] S. Li, B. Liu, Li. Nie, Y. Li, X. Ma, J. Song, Z. Liu, H. Sun, C. Wang, X. Xu, L. Xu, "Comprehensive advanced geological detection system carried on tunnel boring machine," U.S. Patent 9 500 077. Nov. 22, 2016.
[27] S. Gaci, "The use of wavelet-based denoising techniques to enhance the first-arrival picking on seismic traces," *IEEE Trans. Geosci. Remote Sens.*, vol. 52, no. 8, pp. 4558–4563, Aug. 2014, doi: 10.1109/TGRS.2013.2282422.
[28] E. Blias, "Optimization approach to automatic first arrival picking for three-component three-dimensional vertical seismic profiling data," *Geophys. Prospecting*, vol. 60, no. 6, pp. 1024–1029, Nov. 2012, doi: 10.1111/j.1365-2478.2011.01014.x.
[29] J. Wong, L. Han, J. C. Bancrooft, and R. Stewart, "Automatic time-picking of first arrivals on noisy microseismic data," *CSEG*, vol. 1, nos. 1–2, pp. 1–4, 2019.
[30] Y. Chen, G. Zhang, M. Bai, S. Zu, Z. Guan, and M. Zhang, "Automatic waveform classification and arrival picking based on convolutional neural network," *Earth Space Sci.*, vol. 6, no. 7, pp. 1244–1261, Jul. 2019, doi: 10.1029/2018EA000466.
[31] P. J. Hatherly, "A computer method for determining seismic first arrival times," *Geophysics*, vol. 47, no. 10, pp. 1431–1436, Oct. 1982, doi: 10.1190/1.1441291.
[32] J. I. Sabbione and D. Velis, "Automatic first-breaks picking: New strategies and algorithms," *Geophysics*, vol. 75, no. 4, pp. V67–V76, Jul. 2010, doi: 10.1190/1.3463703.
[33] M. E. Murat and A. J. Rudman, "Automated first arrival picking: A neural network approach," *Geophys. Prospecting*, vol. 40, no. 6, pp. 587–604, Aug. 1992.
[34] U. Spagnolini, "Adaptive picking of refracted first arrivals," *Geophys. Prospecting*, vol. 39, no. 3, pp. 293–312, Apr. 1991, doi: 10.1111/j.1365-2478.1991.tb00314.x.
[35] F. Coppens, "First arrival picking on common-offset trace collections for automatic estimation of static corrections," *Geophys. Prospecting*, vol. 33, no. 8, pp. 1212–1231, Dec. 1985, doi: 10.1111/j.1365-2478.1985.tb01360.x.
[36] Y. Ashida, "Seismic imaging ahead of a tunnel face with three-component geophones," *Int. J. Rock Mech. Mining Sci.*, vol. 38, no. 6, pp. 823–831, 2001, doi: 10.1016/S1365-1609(01)00047-8.
[37] C. Chen and G. Wang, "Discussion on the interrelation of various rock mass quality classification systems at home and abroad," *J. Rock Mech. Rock. Eng.*, vol. 21, no. 12, pp. 894–900, 2002.

LICHAO NIE received the Ph.D. degree from the Geotechnical and Structural Engineering Research Center from Shandong University, China, in 2014. He is currently an Associate Professor with the School of Civil Engineering, Shandong University, China. He is mainly engaged in geophysical forward and inversion theory and method, advanced geological prediction method and technology in tunnel, TBM with ahead prediction systems and engineering application, and so on.

WEI ZHOU was born in Jingzhou, Hubei, China, in 1993. He received the master's degree from the China University of Geoscience, China, in 2016. He is currently pursuing the Ph.D. degree with Shandong University. He is mainly engaged in the work of exploration geophysics.

XINJI XU was born in Jining, Shandong, China, in 1990. He received the B.S. degree in city underground engineering and the Ph.D. degree from Shandong University, Jinan, Shandong, in 2012 and 2017, respectively. Since 2017, he has been working as an Assistant Research Fellow with the Geotechnical and Structural Engineering Research Center, Shandong University. His main research interests include engineering geophysical exploration, tunnel forward prospecting, numerical modeling, and seismic data processing.

KAI WANG was born in Yantai, Shandong, China, in 1986. He received the B.S. degree in urban underground space engineering, the M.S. degree in geotechnical engineering, and the Ph.D. degree in disaster prevention and mitigation engineering, from Shandong University, Jinan, in 2010, 2013, and 2017, respectively. Since 2018, he has been working as a Business Director with Qilu Transportation Development Group Company Ltd. His research interests include treatment of geological disasters in underground space of transportation infrastructure and scientific and technological innovation management.

LEI CHEN received the Ph.D. degree from the Geotechnical and Structural Engineering Research Center, Shandong University, China, in 2020. His research interests include engineering geophysical exploration, numerical simulations, as well as tunnel seismic prospecting. He devoted to the application of geophysical methods in engineering.

ZHENGYU LIU received the Ph.D. degree from the Geotechnical and Structural Engineering Research Center, Shandong University, China, in 2018. His research interests include geophysical forward and inversion theory and method.

YAO LI received the Ph.D. degree from the Geotechnical and Structural Engineering Research Center, Shandong University, China, in 2017. He is mainly engaged in ground penetrating radar and research of geophysical instruments.